BMC Plant Biology

RESEARCH Open Access

Revealing cis- and trans-regulatory elements underlying nuclear distribution and function of the *Arabidopsis* histone H2B.8 variant

Janardan Khadka[1,2†], Vikas S. Trishla[1†], Sasank Sannidhi[1], Jeevan R. Singiri[1], Rohith Grandhi[1,3], Anat Pesok[1], Nurit Novoplansky[1], Zachor Adler-Agmon[1,4] and Gideon Grafi[1*]

Abstract

The H2B.8 variant has been diverged from other variants by its extended N-terminal region that possesses a conserved domain. We generated transgenic *Arabidopsis* plants expressing H2B.9 (class I), H2B.5 (class II) and H2B.8 (class III) fused to GFP under the 35 S promoter and studied their nuclear distribution and function. H2B.8-GFP showed peculiar nuclear localization at chromocenters in all cell types examined, while H2B.5-GFP and H2B.9-GFP displayed various patterns often dependent on cell types. H2B variants faithfully assembled onto nucleosomes showing no effect on nuclear organization; H2B.8-GFP appeared as three distinct isoforms in which one isoform appeared to be SUMOylated. Interestingly, transient expression in protoplasts revealed H2B.8 nuclear localization distinct from transgenic plants as it was restricted to the nuclear periphery generating a distinctive ring-like appearance accompanied by nuclear size reduction. This unique appearance was abolished by deletion of the N-terminal conserved domain or when H2B.8-GFP is transiently expressed in *ddm1* protoplasts. GFP-TRAP-coupled proteome analysis uncovered H2B.8-partner proteins including H2A.W.12, which characterizes heterochromatin. Thus, our data highlight H2B.8 as a unique variant evolved in angiosperms to control chromatin compaction/aggregation and uncover cis- and trans-regulatory elements underlying its nuclear distribution and function.

Keywords Histone H2B vaiants, H2B.8, Sumoylation, Chromatin structure, Epigenetics

Introduction

Eukaryotic DNA is packaged into highly organized nucleoprotein complex called chromatin. The fundamental repeating unit of chromatin is the nucleosome, which is composed of 146 base pairs of DNA wrapped around an octamer of core histone proteins H2A, H2B, H3 and H4. A fifth histone, namely, the linker histone H1 binds DNA on its entry and exit from the nucleosomal core particle and is required for the establishment of the 30 nm solenoid fiber and formation of repressive chromatin [31]. The higher order packaging of chromatin influences the accessibility of the genetic material for nuclear processes such as replication, DNA repair and gene expression, which is essential for maintaining the cellular

†Janardan Khadka and Vikas S. Trishla contributed equally to this work.

*Correspondence:
Gideon Grafi
ggrafi@bgu.ac.il
[1]French Associates Institute for Agriculture and Biotechnology of Drylands, Jacob Blaustein Institutes for Desert Research, Ben-Gurion University of the Negev, Midreshet Ben Gurion 84990, Israel
[2]Central Department of Biotechnology, Tribhuvan University, Kirtipur, Nepal
[3]Department of Chemistry, Biochemistry and Physics, Université du Québec à Trois-Rivières, Trois-Rivières, Québec G9A 5H9, Canada
[4]Morris Kahn Marine Research Station, University of Haifa, Haifa 3498838, Israel

© The Author(s) 2024. **Open Access** This article is licensed under a Creative Commons Attribution-NonCommercial-NoDerivatives 4.0 International License, which permits any non-commercial use, sharing, distribution and reproduction in any medium or format, as long as you give appropriate credit to the original author(s) and the source, provide a link to the Creative Commons licence, and indicate if you modified the licensed material. You do not have permission under this licence to share adapted material derived from this article or parts of it. The images or other third party material in this article are included in the article's Creative Commons licence, unless indicated otherwise in a credit line to the material. If material is not included in the article's Creative Commons licence and your intended use is not permitted by statutory regulation or exceeds the permitted use, you will need to obtain permission directly from the copyright holder. To view a copy of this licence, visit http://creativecommons.org/licenses/by-nc-nd/4.0/.

identity [24]. The chromatin can be extensively remodeled by post-translational modifications of histones or incorporation of histone variants making the chromatin structure a dynamic entity [23]. Histone variants are non-allelic protein isoforms encoded by paralogous genes that share a structural domain called the histone fold. Though histone variants have been identified since early research of histone proteins, their diverse roles are not fully understood. The variants of histone H2A and histone H3 are well characterized, and their specialized role have been identified. The histone H2B is the least conserved among the core histone proteins essentially due to the differences in N-terminal regions [12, 20, 21], but much less is known about specialized roles of histone H2B variants.

The model plant Arabidopsis has 11 genes encoding for histone H2B proteins that can be divided into three phylogenetic clusters termed class I, II and III [21]. Class I contains six H2B variants – H2B.1, H2B.2, H2B.3, H2B.4, H2B.9 and H2B.11, class II contains four H2B variants - H2B.5, H2B.6, H2B.7 and H2B.10, and class III contains a single variant H2B.8 (nomenclature of Arabidopsis H2Bs according to Probst et al., [29]. Multiple posttranslational modifications have been detected on Arabidopsis class I H2B variants including acetylation, methylation, and ubiquitination [5], which might modulate their function. Ubiquitylation of lysine residue at the C-terminus (K145) is most studied modification, and in animal it is implicated in establishment of transcriptionally active chromatin [36]. Similarly, in plants, H2B monoubiquitylation has been implicated in gene transcription [8, 18], while deubiquitylation is often associated with gene silencing [38]. In addition, the Arabidopsis H2B variant, H2B.9 appears to be modified by small ubiquitin-like modifier (SUMO) at K142 [33], yet the biological role of this modification is unknown.

The H2B.8 variant was highly diverged from other H2Bs mainly due to presence of an extended N-terminal region with a conserved domain found in the N-terminal extension of H2B.8 orthologs in angiosperms with the core sequence KVVxETVxVxV [20, 21]. In a previous study, Jiang et al. [20] demonstrated the specific expression and nuclear localization of H2B.8 in sperm cells and cotyledons of mature embryos and suggested that H2B.8 might function in chromatin compaction. A recent study highlights a role for H2B.8 in compaction of sperm nuclei *via* chromatin phase separation, which requires the N-terminal extension (IDR, intrinsically disordered region, Buttress et al., [10]. The authors showed that its effect on chromatin aggregation/compaction does not suppress transcription; it may cause decondensation of heterochromatic foci. Furthermore, the expression of H2B.8-scrambled IDR effectively condensed nuclei of tobacco epidermal cells leading to the notion that the effect on chromatin compaction is not mediated through specific sequence motifs within the IDR (Butterss et al., 2022).

Here, we generated transgenic plants expressing a representative member of each H2B class, namely, H2B.9 (class I), H2B.5 (class II) and H2B.8 (class III) and describe variation in nuclear localization of H2B variants and their effect on genome organization and flowering. We showed no effect on genome organization in transgenic plants and highlighted the peculiar nuclear distribution of H2B.8 at heterochromatic chromocenters and its modification by the small ubiquitin-like modifier (SUMO). However, H2B.8-GFP transiently expressed in protoplasts displayed a ring like distribution, induced genome reorganization and reduction in nuclear area, which required the conserved domain at the extended N-terminal region.

Materials and methods

Plant materials

Arabidopsis plants used in the present study include Arabidopsis Landsberg erecta (Ler), *ddm1* (CSHL-GT24941), *cmt3–7* (CS6365, provided by Daphne Autran) as well as transgenic plants carrying H2B variants fused to GFP (see description below) or phyB-GFP (kindly provided by Ferenc Nagy, Medzihradszky et al., [26] were grown in 0.25 L pots containing standard gardening soil composed of peat and perlite (2:1) in a growth room (22 °C±2, 70% humidity) under long day photoperiod (16 h light and 8 h dark) and light intensity of ~ 150 µmol m^{-2} s^{-1}.

Cloning of histone H2B genes and generation of H2B-GFP transgenic lines

Genomic DNA was extracted from *Arabidopsis thaliana* (Ler ecotype) and used as a template for PCR amplification of *H2B.5* (At2g37470), *H2B.8* (At1g08170) and *H2B.9* (At3g45980) coding sequences using primers (supplemental Table 1) flanked with *Bam*HI and *Sma*I sites at the 5' and 3' ends, respectively. Parental plasmid *pUC19-35 S-MBD5-GFP* [47] was cut by the *Bgl*ll-*Sma*I to replace *MBD5* sequence by *Bam*HI-*Sma*I fragment of *H2B.5*, *H2B.8 and H2B.9* genes that yielded *pUC19-35 S-H2B-GFP* variants. Each of the ligated product was transformed into *E. coli* Top10 competent cells and grown on LB agar media supplemented with 100 mg/L Ampicillin. Then, colonies grown on the selective media were tested for presence of desired insert by colony PCR using M13/pUC and cpGFP primers (Table S1). We used In-Fusion Cloning kit (Takara) to generate pUC19-35 S-H2B.8-DCD-GFP in which the first 26 amino acids including the CD were deleted from the N-terminus of H2B.8. Briefly, pUC19-35 S-H2B.8-GFP was used as a parental plasmid and primers H2B.8DCD-F and GFP-R (Table S1) according to the manufacturers' protocol. Plasmid DNAs were extracted from positive clones using Presto mini plasmid

kit (Geneaid) and correctness of insert sequences was checked by sequencing. For generation of transgenic plants, the 35 S-H2B-GFP DNA sequences were excised out by *Xho*I and *Pst*I and subcloned into the same sites of *pGreen*II0229. The *pGreenII0229* constructs with *pSOUP* vector were co-transformed into electrocompetent *Agrobacterium tumefacien* (GV3101 strain) by electroporation and selected in LB media plates supplemented with Kanamycin (50 mg/L), Gentamicin (50 mg/L), Tetracyclin (10 mg/L). The *Agrobacterium* clones were transformed into *Arabidopsis thaliana* (Ler ecotype) by floral dip method [49]. The transformant seedlings were screened by spraying Basta herbicide and at least two independent insertion lines (GFP positive) were selected for the experiments. Calluses were prepared from transgenic plants by incubating leaf explants on MS medium [27] supplemented with B5 salts, 3% sucrose, 0.5 mg/L 2,4-D, and 0.5 mg/L benzylaminopurine (BAP).

Nuclei isolation and salt extraction

Nuclei were isolated using NIB buffer (10 mM MES-KOH, pH 5.5, 0.2 M sucrose, 2.5 mM EDTA, 2.5 mM dithiothreitol, 0.1 mM spermine, 10 mM NaCl, 10 mM KCl, 0.15% Triton X-100) from leaves of three to four-week-old Arabidopsis plants expressing H2B variants-GFP essentially as described [35]. Salt extraction of nuclear proteins was performed as described [30]. Briefly, the nuclei were washed with Buffer N and incubated with 75 µl sucrose-deficient Buffer N containing 75, 350, 600 and 1000 mM NaCl. After a 30 min incubation on ice, the samples were centrifuged at 12,000 g for 10 min at 4 °C. The soluble (S) fraction was collected, and the pellet (P) was resuspended in 75 µl of SDS-loading buffer. Equivalent samples from S and P fractions were resolved on 15% SDS-PAGE and immunoblotted using anti-GFP (Genescript, USA) and anti-H3K4me2 antibodies (Cell Signaling Technology, Danvers, MA, USA).

Micrococcal nuclease (MNase) assay, chromatin fractionation and immunoblotting

MNase assay was performed as described [51]. Chromatin fractionation was performed essentially as previously described [14]. Briefly, nuclei were resuspended in 100 µl of Buffer N [30] and digested with 90 units of micrococcal nuclease (NEB) at 37 °C for 10 min. The digested nuclei were cooled on ice for 10 min and centrifuged at 10,000 g for 10 min at 4 °C. The supernatant (S1) was removed by aspiration and the pellet was resuspended in 100 µl of ice-cold 2 mM EDTA, pH 8.0. The samples were incubated on ice for 10 min, centrifuged as above and the supernatant (S2) was collected. The pellet (P) was resuspended in 100 µl of SDS-loading buffer. Equivalent samples were resolved on 15% SDS-PAGE and immunoblotted using anti-GFP (Genescript, USA) or anti-H2B (D2H6, Cell Signaling) and anti-H2Bubi (Millipore, clone 56). A portion of the digested nuclei was used for DNA preparation as described [51].

Analysis of H2B.8 SUMOylation was performed on nuclear extract derived from leaves of transgenic plants expressing H2B.8-GFP. Accordingly, nuclei were prepared from 6 g leaves with NIB buffer (10 mM MES-KOH, pH 5.5, 0.2 M sucrose, 2.5 mM EDTA, 2.5 mM dithiothreitol, 0.1 mM spermine, 10 mM NaCl, 10 mM KCl, 0.15% Triton X-100) and extracted with NETN buffer containing protease inhibitor cocktail (Sigma) followed by water bath sonication. Homogenates were centrifuged at high speed (14,000 x g, 10 min, 4°C), the supernatant was collected and subjected to GFP-TRAP procedure according to the manufacturer's protocol. Immunoprecipitates were resolved on 12% SDS/PAGE and immunoblotted using anti-GFP (Genescript, USA), anti-UBQ11 (Agrisera) or anti-SUMO1/SUMO3 (Agrisera).

Protoplast preparation and transformation

Transient expression in protoplasts was performed essentially as described [46]. Arabidopsis leaves were incubated in a cell wall degrading solution containing 1.5% cellulase, 0.5% macerozyme, 0.4 M mannitol, 20 mM KCl, 20 mM MES, 10 mM $CaCl_2$, and 0.1% BSA, placed in a vacuum for 20 min, and then shaken for 90–120 min at 50 rpm. The protoplasts were then filtered through a 180-µm mesh, diluted with 1 volume of W5 (150 mM NaCl, 125 mM $CaCl_2$, 5 mM KCl, and 2 mM MES) and pelleted by centrifugation (Room temperature, 2 min at 300 x g). The protoplasts were re-suspended in W5 solution and incubated for 30 min on ice, before being centrifuged again and resuspended in 100 µl of MMg solution containing, 0.4 M mannitol and 15 mM $MgCl_2$. Plasmid DNA (5–20 µg) was added to protoplasts and equal volume of 40% PEG solution (in 0.2 M mannitol and 0.1 M $CaCl_2$) and the mixture was incubated for 15–30 min. Two volumes of W5 were added to each sample, centrifuged for 2 min, re-suspended in 1 ml of W5, and then incubated at room temperature for 16–24 h. Protoplasts were inspected under a confocal microscope (ZEISS, LSM980) to visualize the GFP signal.

Identification of H2B.8-GFP partner proteins

To identify potential proteins associated with H2B.8 we performed GFP-TRAP on total proteins extracted from Arabidopsis transgenic plants expressing H2B.8-GFP; extract derived from transgenic plants expressing phytochrome B-GFP (phyB-GFP) was used as a reference. Accordingly, total proteins were extracted from Arabidopsis leaves using NETN buffer (100 mM NaCl, 1 mM EDTA, 20 mM Tris, pH 8, and 0.5% NP-40) supplemented with a protease inhibitor cocktail (Sigma, St. Louis, MO, USA). Protein concentration was determined

by Bradford reagent. GFP-TRAP was performed with 1 mg of total proteins (3 replicates for H2B.8-GFP and 2 replicates for phyB-GFP) according to the manufacturer's protocol and immunoprecipitates were subjected to proteome analysis. Proteome analysis was performed by the proteomic services of the Smoler Protein Research Center at the Technion, Haifa, Israel using LC-MS/MS on LTQ Orbitrap (ThermoFisher Scientific, Waltham, MA, USA; https://proteomics.net.technion.ac.il/proteomic-services/ accessed on 11 May 2021). Protein identification and quantification were done using MaxQuant, using *Arabidopsis thaliana* proteins from Uniport as a reference. Quantification and normalization were performed using LFQ method. Subsequent bioinformatics analysis was performed by using Perseus software [40]. Proteins marked as "contaminant "and "only identified by site" were filtered out. In an additional step, only proteins in which at least one of the groups had at least 2 non-zero replicates and proteins having at least 2 peptides were retained. A protein was considered H2B.8-partner protein if it is a nuclear protein and had zero value in the reference (PhyB-GFP) replicates.

Results

Nuclear distribution of H2B variants

Transgenic plants carrying H2B variants, H2B.5, H2B.9 and H2B.8 fused to GFP under the 35 S promoter were inspected under a confocal microscope. Transgenic plants expressing H2B.8-GFP showed peculiar localization in the nucleus where it was restrictively localized at chromocenters in all cell types examined including cotyledons, trichomes and callus cells (Fig. 1). Also, in the shoot and the root apical meristems H2B.8-GFP was localized to chromocenters as suggested by their colocalization with the intensely DAPI-stained chromocenters (Supplemental Fig. 1). On the other hand, H2B.5-GFP and H2B.9-GFP displayed nuclear localization distinct from that of H2B.8-GFP and often dependent on cell type (Supplemental Fig. 2). Accordingly, both H2B.5-GFP and H2B.9-GFP showed a spongy-like pattern in cauline and rosette leaves, with H2B.9-GFP often showing accumulation at two perinucleolar chromocenters in rosette leaf and cotyledons, while H2B.5-GFP showing punctuated distribution; Both H2B.5 and H2B.9 are more dispersed in guard cell nuclei.

Genome organization in transgenic plants

Micrococcal nuclease digestion of nuclei prepared from wild type and transgenic plants showed that the pattern of nucleosomal ladder in transgenic plants overexpressing H2B variants was like the pattern of wild type plants, suggesting that overexpression of H2B variants did not affect the general organization of the *Arabidopsis* genome (Fig. 2A).

The strength of the interaction between H2B variants and chromatin was assessed by extracting nuclei from rosette leaves of transgenic plants with increasing concentrations of NaCl (Fig. 2B). After 30 min incubation on ice, the soluble (S) and the insoluble pellet (P) fractions were run on SDS/PAGE followed by immunoblotting with anti-GFP. Initial experiments with nuclei prepared from transgenic plants expressing H2B.5-GFP and H2B.9-GFP showed (Supplemental Fig. 3) that under 75 mM NaCl, the examined H2B variants were found

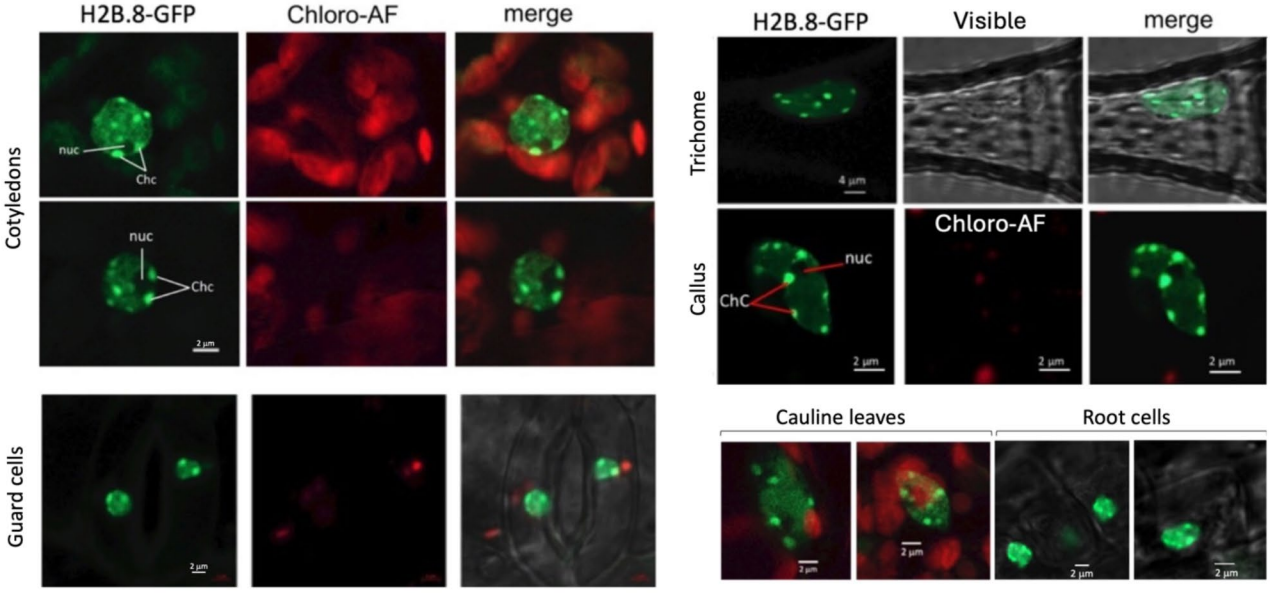

Fig. 1 Sub-nuclear localization of H2B.8-GFP in the indicated organs and cell types in transgenic plants. Note H2B.8-GFP is restrictively localized to chromocenters (ChC) in all cell types examined. Nuc, nucleolus. Chc, chromocenters. Chloro-AF, Chloroplast AutoFluorescence

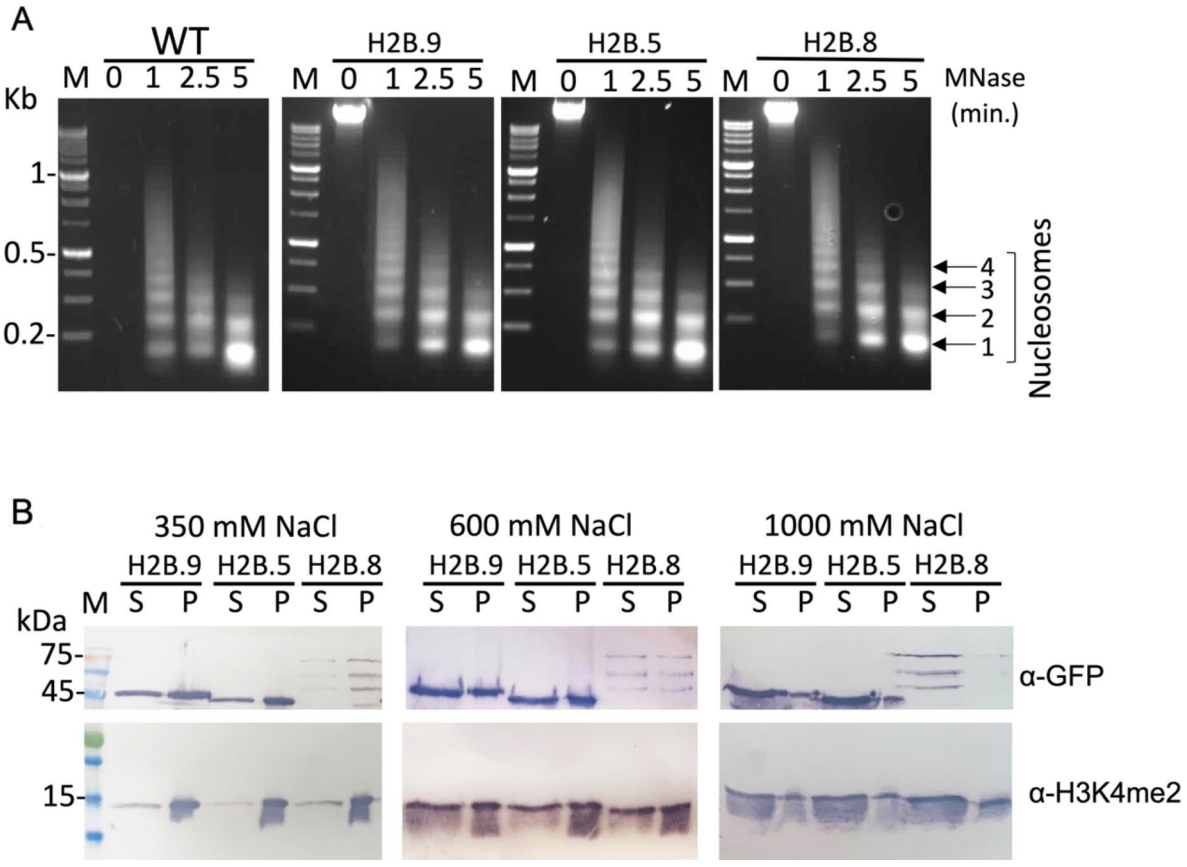

Fig. 2 Genome organization in transgenic plants, micrococcal nuclease assay and salt extraction. **(A)** Expression of H2B variants under the 35 S promoter had no effect on genome organization. Nuclei prepared from WT and H2B variants expressing plants were subjected to micrococcal nuclease (MNase, 300 units / ml) for 1, 2.5 and 5 min, DNA was extracted and run on 1.5% agarose gel. M, DNA size markers given in kilobase (kb). DNA fragments protected by 1–4 nucleosomes are marked by arrows. Note, no recovery of WT genomic DNA at time 0 resulted from DNA extraction error. **(B)** Salt extraction of nuclei. Nuclei derived from rosette leaves of transgenic plants were extracted with NIB buffer containing increasing concentration of NaCl (350, 600 and 1000 mM). After incubation on ice for 30 min, the soluble fraction (S) was separated from the pellet (P) and equivalent samples from each fraction were subjected to 15% SDS/PAGE followed by western blotting using anti-GFP for detection of H2B variants and anti-H3K4me2 as a reference protein. Note the membrane was cut into two parts, the upper containing proteins above 40 kDa was probed with αGFP and the lower part with αH3K4me2. The EZblue staining of the gel is given in supplemental Fig. 4. M, protein molecular weight markers given in kDa

exclusively in the pellet, suggesting that H2B variants are strongly associated with chromatin similarly to the reference dimethylated histone H3K4 (H3K4me2). Increasing concentration to 350 mM resulted in the release of a small fraction of H2B variants into the soluble fraction (S) (Fig. 2B; supplemental Fig. 3), which was increased with increasing NaCl concentration; under 1 M NaCl most H2B variants were found in the soluble fraction similarly to the reference histone H3K4me2 (Fig. 2B). Interestingly, H2B.8-GFP appears as three distinct isoforms with molecular masses ranging from ~ 54 to 75 kDa (Fig. 2B).

These three H2B.8-GFP isoforms were recovered following treatment of nuclei with high concentration of micrococcal nuclease (MNase) in a chromatin fractionation assay. In this assay, a typical nucleosomal ladder with mononucleosomes enriched in S1 fraction and oligo-nucleosomes in S2 fraction were observed for wild type and transgenic plants (Fig. 3A). Notably, all examined H2B-GFP variants were recovered (GFP antibody) mostly in S1 and S2 fractions similarly to the recovery of the reference endogenous H2B protein (Fig. 3B). Yet, running chromatin fractionation assays with low concentrations of MNase showed slight differences in recovery of H2B variants. Accordingly, we found that a small fraction of H2B.5, but not H2B.9, H2B.8 or the reference histone H3K4me2, was recovered in S1 fraction under 10 units of MNase (Supplemental Fig. 5A). Similarly, under 45 units of MNase, H2B.5 but not H2B.9 was recovered in S1 fraction (Supplemental Fig. 5B). Unexpectedly, in this assay the reference ubiquitylated H2B (H2Bubi), often implicated in open chromatin appeared mostly associated with the insoluble, pellet fraction, and a small fraction

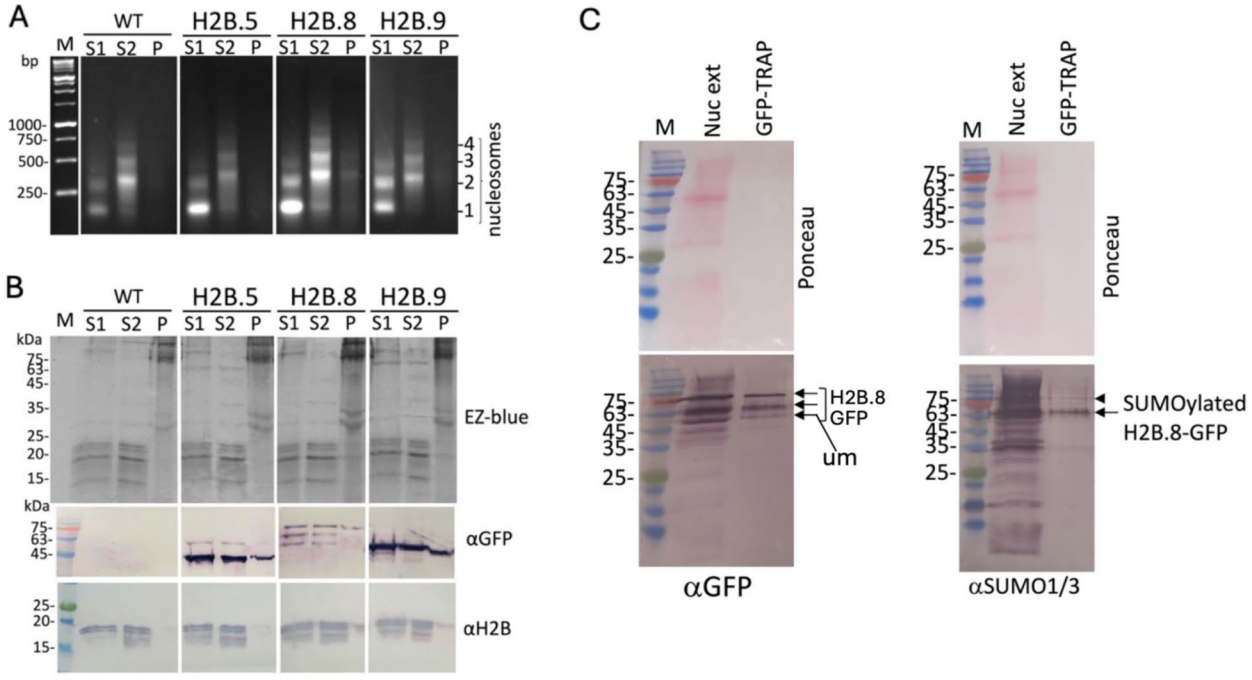

Fig. 3 H2B.8 is SUMOylated. **(A)** The nucleosomal ladder of MNase-digested nuclei. Nuclei prepared from 6 g rosette leaves of WT and transgenic plants expressing H2B variants fused to GFP were digested with 150 units of MNase and processed to yield the soluble fractions S1 and S2 and the pellet (P) fraction. DNA was prepared from S1, S2 and the pellet (P) following MNase digestion and separated on 1.5% agarose gel and stained with ethidium bromide. The position of DNA fragments protected by 1–4 nucleosomes is indicated. The molecular weight markers are indicated in basepair on the left. **(B)** Equivalent samples from S1, S2, and P fractions were resolved by 15% SDS-PAGE and immunoblotted using anti-GFP (aGFP) and anti-H2B (aH2B). M, protein molecular weight markers given in kDa. Note the upper panel in B is gel staining with EZ-blue after transfer to a membrane. Also, the membrane was cut into two halves, the upper above 35 kDa was probed with aGFP, and the lower half with the reference aH2B. **(C)** Nuclear extract from transgenic plant expressing H2B.8-GFP was subjected to immunoprecipitation using GFP-TRAP followed by immunoblotting using anti-GFP (left panel) or anti-SUMO1/SUMO3 (right panel). Um indicates unmodified H2B.8-GFP. Nuc ext is the input nuclear extract. M, protein molecular weight markers (kDa)

of H2Bubi was recovered in the S1 and the S2 fractions (Supplemental Fig. 5B).

H2B.8-GFP is SUMOylated in leaves of transgenic plants

Based on the molecular mass of the three isoforms recovered from H2B.8-GFP expressing plants, we suspected that H2B.8-GFP might be modified by ubiquitin or more likely by small ubiquitin-related modifier (SUMO) proteins. To examine this possibility, nuclei prepared from leaves of H2B.8-GFP expressing plants were sonicated or extracted with high salt concentration (1 M NaCl) in NETN buffer to obtain the nuclear extract, which was subjected to GFP-TRAP. Immunoprecipitates were run on 12% SDS/PAGE and immunoblotted using either anti-GFP, anti SUMO1/SUMO3 (a mixture of antibodies raised to *Arabidopsis* SUMO1 and SUMO3, Agrisera) or anti-ubiquitin. As can be seen (Fig. 3C, left panel), anti-GFP recovered three protein bands in the range of 54 to 75 kDa, that represent H2B.8-GFP isoforms. Thus, while the 54 kDa isoform represents the unmodified H2B.8-GFP the other 2 isoforms appear to be modified. Probing the membrane with anti-SUMO1/SUMO3 recovered a major isoform of about 64 kDa and a faint isoform at about 75 kDa (Fig. 3C, right panel), suggesting that H2B.8 is SUMOylated in plant cells. No H2B.8-GFP isoform could be recovered with anti-ubiquitin (Supplemental Fig. 6).

Nuclear distribution of H2B.8-GFP in protoplasts

A recent study suggested a role for H2B.8 in compaction of sperm nuclei *via* chromatin phase separation, due to the N-terminal IDR [10]. In transgenic plants H2B.8 was localized to chromocenters showing no apparent function in chromatin aggregation. We wanted to examine the hypothesis that H2B.8 might induce chromatin aggregation following exposure to stress such as protoplasting. To this end, leaves of H2B.8-GFP transgenic plants were used for protoplast isolation followed by incubation in W5 or MMg medium, which contains 15 mM $MgCl_2$. Notably, the formation of chromatin aggregates is often triggered under specific conditions where the concentration of $MgCl_2$ plays central role [10, 16]. Four basic types of nuclear distribution could be identified in protoplasts (Fig. 4A and B), namely, chromocentric as in leaf cells (type A and 'a'), ring-like distribution (type B) and type C where H2B.8-GFP was evenly dispersed within the

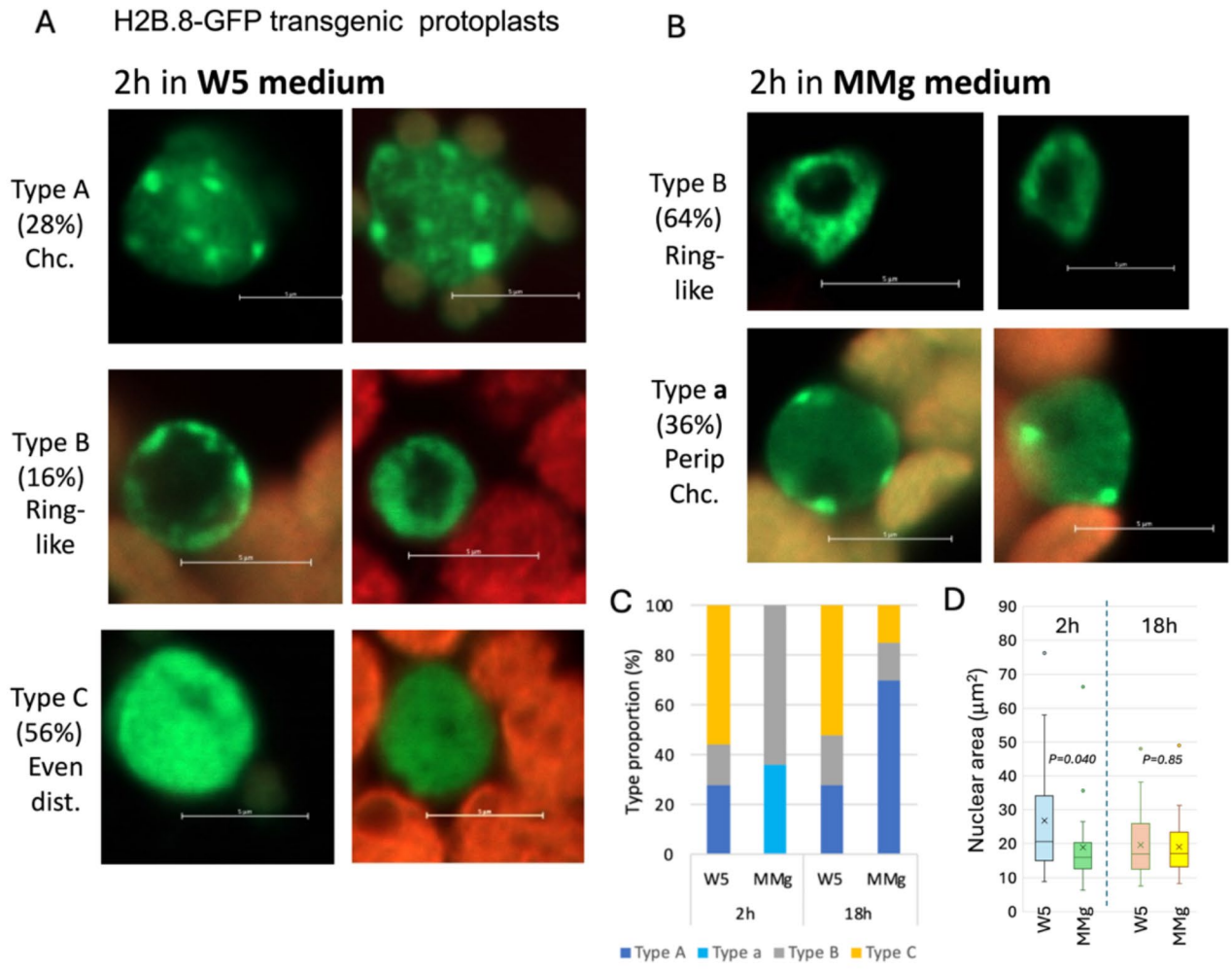

Fig. 4 H2B.8-GFP nuclear distribution is changed following protoplast isolation in an incubation medium dependent manner. **(A)** Nuclear distribution of H2B.8-GFP following protoplasts preparation and incubation for 2 h in W5 medium. Three distribution types were recorded, A (chc, chromocentric), B (ring-like) and C (even distribution). The proportion of each type is given in brackets ($n=25$). **(B)** Incubation in MMg medium demonstrating two types 'a' (perinuclear chc.) and B. The proportion of each type is given in brackets ($n=25$). **(C)** The proportion of distribution types in W5 and MMg solution after 2 and 18 h of incubation. **(D)** A boxplot representing the average nuclear area of protoplasts incubated in W5 or MMg medium ($n=25$) for 2 h and 18 h. x in each box represents the mean and the horizontal line represents the median. Statistical analysis was performed by student's unpaired *t-test* (GraphPad software)

nucleus. The proportion of these types was affected by the incubation medium (W5 vs. MMg) and by the incubation time (2 h vs. 18 h; Fig. 4C). Thus after 2 h incubation in W5 most protoplasts showed even distribution in the nucleus (type C, 56%), 28% showed chromocentric localization as in leaves of transgenic plants (type A) and 16% showed a ring like distribution (type B). Most protoplasts incubated in MMg displayed type B distribution (64%) and 36% type 'a' after 2 h incubation. Incubation for 18 h showed no significant changes in nuclear distribution in W5 protoplasts, but substantial changes in MMg protoplasts. Accordingly, most MMg protoplasts (70%) showed type A nuclear distribution after 18 h incubation. Furthermore, we calculated the average nuclear area and found significant reduction in nuclear area after 2 h in MMg protoplasts as compared to W5; no difference in nuclear area between MMg and W5 could be seen after 18 h incubation (Fig. 4D) implying that H2B.8-GFP might transiently induce compaction of chromatin in medium containing Mg^{2+}.

The N-terminal conserved domain is required for H2B.8 nuclear distribution and chromatin aggregation

We next examined the role of the N-terminal extension in H2B.8-GFP nuclear localization. As mentioned above, H2B.8 has been highly diverged from other H2B variants having an extended N-terminal tail of about 120 amino acids containing a highly conserved domain

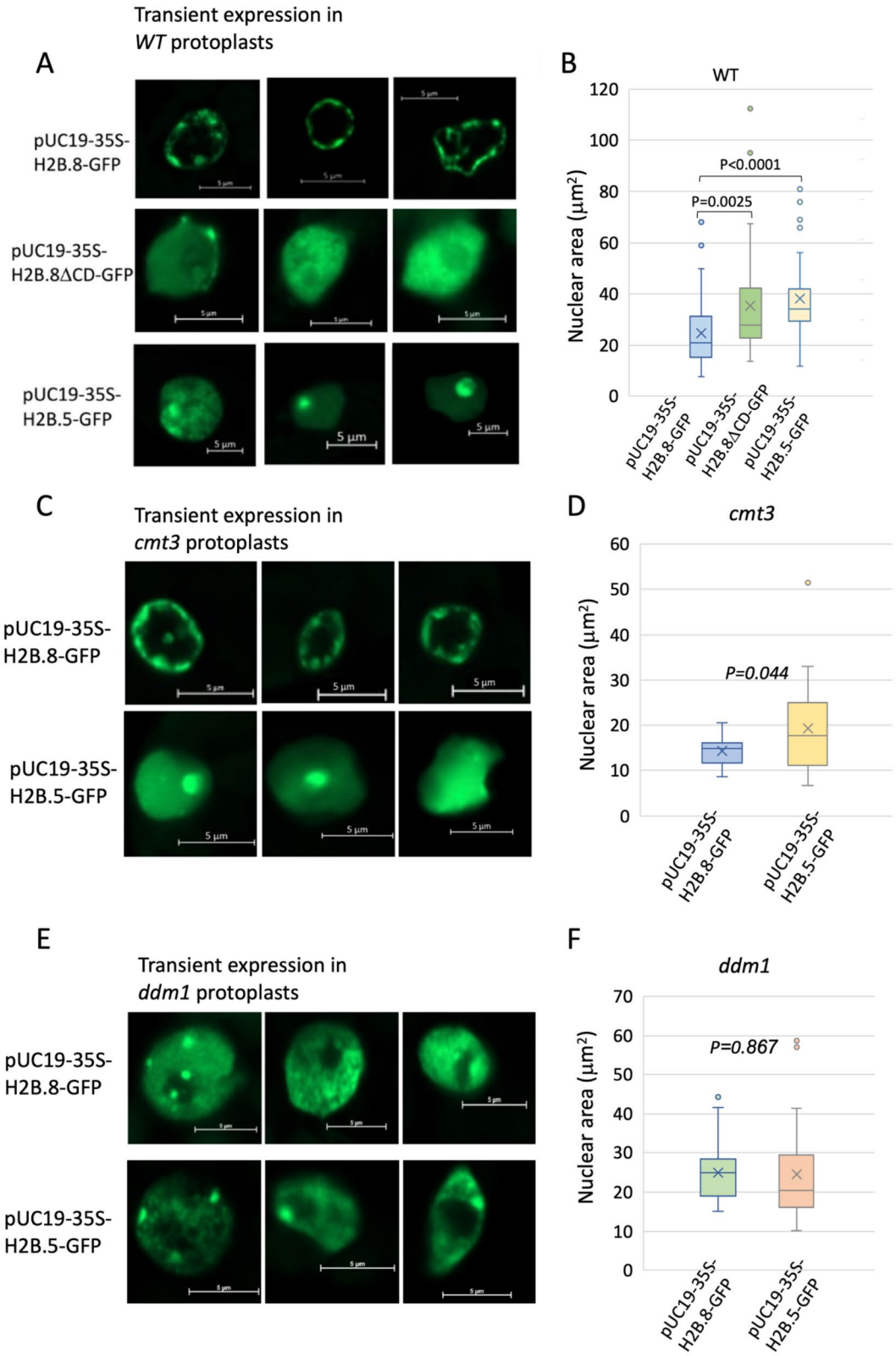

Fig. 5 (See legend on next page.)

(See figure on previous page.)

Fig. 5 The N-terminal conserved domain (CD) and DDM1 are required for H2B.8 peculiar nuclear distribution and function in protoplasts. **(A)** Protoplasts were transformed with pUC19-35 S-H2B.8-GFP, pUC19-35 S-H2B.8DCD-GFP, and as a reference, pUC19-35 S-H2B.5-GFP and inspected under a confocal microscope. Scale bars are the authentic scale bar for each nucleus. Note the ring shape nuclear distribution of H2B.8-GFP in protoplasts and its disruption when the CD is deleted (DCD). **(B)** A boxplot representing the nuclear area of protoplasts transformed with the indicated constructs ($n = 50$; for H2B.5-GFP $n = 44$). x in each box represents the mean and the horizontal line represents the median. Statistical analysis was performed by student's unpaired *t-test* (GraphPad software). **(C, E)** pUC19-35 S-H2B.8-GFP and pUC19-35 S-H2B.5-GFP were transformed with into *cmt3* and *ddm1* protoplasts and inspected under a confocal microscope. Note the ring shape nuclear distribution of H2B.8-GFP in *cmt3* protoplasts (c) and its disruption in *ddm1* protoplasts (e). **(D, F)** Boxplots representing the nuclear area of *cmt3* (d, $n = 23$) and *ddm1* (f, $n = 38$) protoplasts transformed with the indicated constructs. x in each box represents the mean and the horizontal line represents the median. Statistical analysis was performed by student's unpaired *t-test* (GraphPad software)

(H2B.8-CD) found in all examined H2B.8-like proteins in angiosperm with the core sequence of KVVxETVxVxV [20, 21]. To assess the function of H2B.8-CD in nuclear localization, we generated H2B.8 mutant in which the 26 amino acids from the N-terminus that include the CD were deleted. Thus, H2B.8-GFP, H2B.8ΔCD-GFP as well as H2B.5-GFP subcloned into pUC19 downstream from the 35 S promoter (pUC19-35 S::H2B.8-GFP; pUC19-35 S::H2B.8DCD-GFP; pUC19-35 S::H2B.5-GFP) were transiently transformed into *Arabidopsis* protoplasts and visualized after 18 h under a confocal microscope. Results showed (Fig. 5A) that H2B.8-GFP assumed nuclear distribution which is profoundly different from its nuclear distribution in leaves of transgenic plants. Thus, it shows prominent localization at the nuclear periphery generating a distinctive ring-like appearance where chromatin dots often appear connected. This unique subnuclear localization/organization was completely abolished in H2B.8-DCD, showing a high proportion of nuclei with even distribution within the nucleus, suggesting that this domain is required for H2B.8 nuclear distribution and function. H2B.5-GFP showed two types of nuclear localization, namely, about half of transformed protoplasts showed nucleolar localization and half of protoplasts displayed dispersed distribution in the nucleus (Fig. 5A and supplemental Fig. 7). We observed a significant reduction in nuclear size in protoplasts expressing H2B.8-GFP compared to protoplasts expressing H2B.8DCD-GFP or expressing H2B.5-GFP (Fig. 5B).

To assess the involvement of epigenetic modifiers in nuclear distribution and function of H2B.8-GFP, we performed transient expression in protoplasts derived from *chromomethylase3* (*cmt3)* mutant, displaying reduction in non-CG methylation [4, 25], and from decrease in DNA methylation1 (*ddm1)* mutant that shows significant reduction in DNA and histone H3K9 methylation, and consequently impairment in chromocenter assembly [37, 42]. Results showed no change in H2B.8-GFP nuclear distribution and function in *cmt3* (Fig. 5C and D) but impairment in *ddm1* protoplasts (Fig. 5E and F).

Identification of H2B.8 interacting partners: GFP TRAP analysis

To gain insight into the mechanisms underlying H2B.8 nuclear distribution we sought to identify potential H2B.8 associated proteins. To this end, total proteins extracted from transgenic plants expressing H2B.8-GFP were subjected to GFP-TRAP followed by proteome analysis (Supplemental Table S2). As a control we used total proteins extracted from transgenic plants expressing PHYB-GFP (Supplemental Table S2), which is known to translocate to the nucleus under light conditions [34, 44]. Only proteins in which at least one of the groups (H2B.8-GFP, PhyB-GFP) had at least 2 non-zero replicates were retained. We identified 330 proteins that have at least 2 peptides. Nuclear proteins (as determined by UniProt) showing zero value in two replicates of PhyB-GFP and 2 non-zero replicates in H2B.8-GFP immunoprecipitates were considered as potential H2B.8-interacting proteins. This analysis revealed (Table 1) several interesting nuclear proteins associated with H2B.8, namely, H2A.W.12 (At5g02560), commonly localized to constitutive heterochromatin [45], gamma histone variant H2A.X.3 (At1g54690), involved in DNA damage repair and AT hook motif-containing protein (At1g48610) whose function is unknown. In addition, other interesting proteins include histone H1.2 and H2B.10, which were excluded because of their identification by a single peptide.

Overexpression of H2B variants affect flowering time

Modification of H2B by ubiquitiation has been implicated in controlling flowering time [11, 15]. We thus investigated which of the studied H2B variants has the most prominent effect on flowering. The transgenic *Arabidopsis* plants overexpressing H2B.5-GFP, H2B.8-GFP and H2B.9-GFP under the 35 S promoter grew normally with no notable phenotypic abnormalities. However, flowering was significantly accelerated in plants overexpressing H2B.5-GFP and H2B.9-GFP (Fig. 6A) where flowering occurs with an average of 8 rosette leaves compared to ~ 11 and 12 in H2B.8-GFP and wild type plants, respectively (Fig. 6B). We obtained a mixed population of *h2b.5* T-DNA insertional mutant from the ABRC collection (SALK_003306). Homozygous *h2b.5* plants displayed late flowering compared to wild type plants (Fig. 6C).

Table 1 A list of nuclear proteins co-immunoprecipitated with H2B.8-GFP in a GFP-TRAP assay. Plants expressing PHYB-GFP were used as a reference

Protein ID	Gene ID	Protein name	PHYB-GFP-1	PHYB-GFP-2	H2B.8-GFP 1	H2B.8-GFP 2	H2B.8-GFP 3
P14713	At2g18790	Phytochrome B	1.49E + 09	5.41E + 09	0.00E + 00	0.00E + 00	0.00E + 00
Q9SGE3	At1g08170	H2B.8	0.00E + 00	0.00E + 00	3.06E + 09	1.59E + 09	4.51E + 07
Q9S9K7	At1g54690	H2A.X.3	0.00E + 00	0.00E + 00	1.25E + 08	7.86E + 07	0.00E + 00
F4KCF4	At5g02560	H2A.W.12	0.00E + 00	0.00E + 00	6.43E + 07	2.42E + 07	0.00E + 00
Q94AD1	At1g48610	AT hook motif-protein	0.00E + 00	0.00E + 00	4.56E + 07	2.13E + 06	0.00E + 00

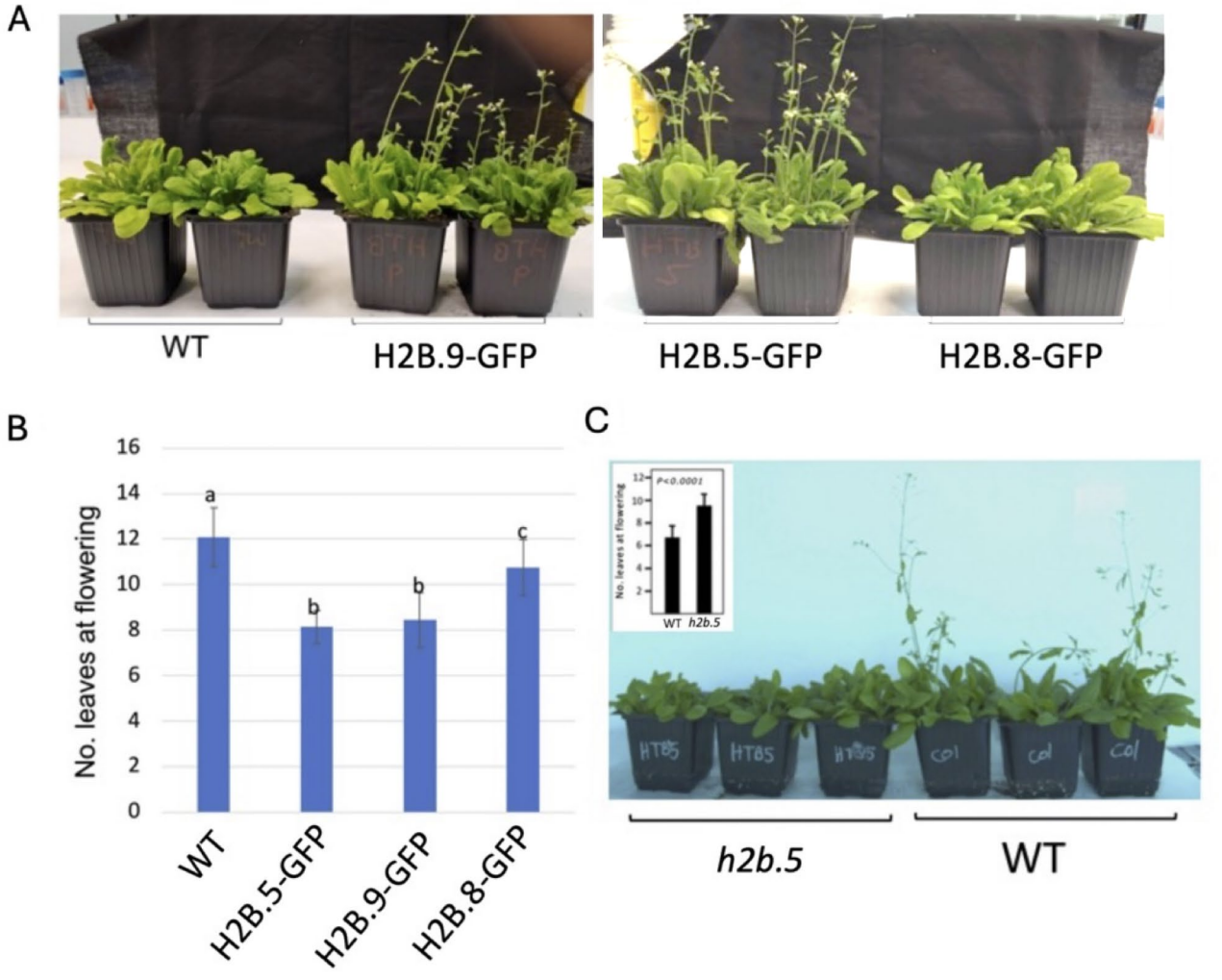

Fig. 6 Overexpression of H2B.9-GFP and H2B.5-GFP accelerates flowering. **(A)** Flowering of WT and the indicated transgenic lines were recorded 6 weeks after sowing under 22°C/16°C (day/night) thermoperiod and 16 h/8 h (day/night) photoperiod. **(B)** Average number of rosettes leaves at the time of flowering in WT and transgenic lines ($n = 50$). Bars represent the standard deviation. Statistical significance was performed by a One-Way ANOVA Calculator, Including Tukey HSD (Social Science Statistics). Different letters indicate statistically significant differences between lines ($p < 0.05$). **(C)** Flowering is delayed in *h2b.5* mutant. Inset is the number of leaves at flowering for WT and *h2b.5* mutant ($p < 0.0001$)

Discussion

Nuclear distribution of H2B variants

The dynamic of chromatin structure and its accessibility for various nuclear processes such as transcription and repair are modulated by DNA and histone modifications as well as by histone variants. Thus, in plants and animals each group of core histone proteins is composed of multiple variants that commonly share the histone fold but showed divergence at the N- and C-terminal tails. Among the core histone proteins, the H2B variants in plants are the least investigated. Transgenic Arabidopsis plants expressing a member of each H2B class fused to GFP, namely H2B.9 (class I), H2B.5 (class II), and H2B.8 (class III) display peculiar subnuclear localization.

Particularly, H2B.8-GFP showed restrictive localization at chromocenters in all cell types examined, suggesting that it may be involved in establishment/maintenance of heterochromatin. Notably, H2B.8 has been shown to be specifically expressed in sperm cells and in mature seeds (Jiang at al., 2020), both have been shown to acquire compact chromatin [7, 10, 41]. Similar chromocentric localization of H2B.8 was demonstrated in Jiang et al. [20], where closer examination of the published data revealed that H2B.8-RFP is not evenly distributed in the embryonic cotyledon nuclei but rather showing spotted distribution, suggesting localization at chromocenters. Interestingly, protoplasts derived from H2B.8-GFP expressing transgenic plants showed distinct nuclear distribution which is dependent on the incubation medium and the time of incubation. Thus, H2B.8-GFP displayed a ring type appearance accompanied by reduction in nuclear size in most protoplasts following short term incubation in MMg medium but not in W5, suggesting that Mg^{2+} may be necessary for H2B.8 to induce chromatin aggregation in vivo, which is reduced significantly after long term incubation. Notably, Buttress et al. [10] demonstrated, in vitro, the capacity of H2B.8 to induce phase-separation of nucleosomal arrays in the absence of salt, yet this capacity has not been described in vivo. There are multiple reports demonstrating the dependency of nucleosome array folding and aggregation on the charge and concentrations of cations (mainly Mg^{2+} and Na^{+}) in solution; these studies were mainly performed in vitro (Reviewed in Hansen et al., [16] and the relevance to the in vivo condition requires further investigation. Interestingly, while compaction of chromatin brings about transcriptional repression, formation of aggregates did not block gene transcription suggesting that chromatin aggregates are accessible to the transcriptional machinery and are biologically significant [10, 39]. Furthermore, chromatin distribution at the nuclear periphery although often is highly condensed, non-accessible chromatin may contain both active and repressed regions [1]. It should be mentioned that certain histone posttranslational modifications were found to attenuate chromatin aggregation including histone acetylation and H2B ubiquitylation demonstrating that formation of chromatin aggregates/condensates is highly dynamic and subjected to control by multiple factors [16].

H2B.8 function requires the N-terminal conserved domain

Transient expression into protoplasts revealed the function of H2B.8 and its derivatives in chromatin aggregation. Accordingly, pUC19-35 S-H2B.8-GFP transiently transformed into WT Arabidopsis protoplasts showed distinct localization to multiple spots arranged as a ring around the nuclear periphery. This is not seen in protoplasts transformed with MBD7-GFP that showed distinct nuclear localization at chromocenters [47, 48]. This suggests that expression of H2B.8-GFP in protoplasts induces genomic reorganization whereby H2B.8-GFP containing chromatin are tethered to the nuclear periphery by yet an unknown mechanism(s). Alternatively, H2B.8, through its IDR may induce chromatin aggregation [10] that is further assembled to the nuclear periphery, probably in a lamin-like protein-dependent manner [19]. Buttress et al. [10] suggested that chromatin phase separation/aggregation requires the IDR independently of specific sequence motifs (i.e., the CD), although many H2B.8 orthologs in angiosperm share this motif. The analysis of H2B.8 with ESpritz IDR prediction tool [43] shows that the N-terminal extension (i.e., IDR) is not entirely disordered but composed of an ordered region overlapping the CD (supplemental Fig. 8). Notably, while IDRs may drive phase separation, not all disordered protein regions have the intrinsic capacity for driving phase separation; "only a subset of IDRs has a strong enough driving force to undergo phase separation that is physiologically relevant" [6]. Thus, our results clearly showed that H2B.8 function in genome aggregation in protoplasts requires the N-terminal CD since deletion of the CD abolished H2B.8 nuclear distribution and function. Yet, while the CD is required, it may not be sufficient for H2B.8 nuclear distribution and function. We assume that the IDR might be required as well [10], a matter we currently study.

H2B.8 function and associated proteins

The mechanism(s) involved in H2B.8 localization and function at chromocenters in transgenic plants may be uncovered by the identification of H2B.8 partner proteins. Using GFP-TRAP of total proteins extracted from H2B.8-GFP transgenic plants we recovered several potential H2B.8-partner proteins. This analysis revealed a nuclear protein often associated and involved in establishment of heterochromatin, namely, H2A.W.12. The three H2A.W variants in *Arabidopsis*, namely, H2A.W.6, H2A.W.7 and H2A.W.12 all characterize heterochromatin often localized to chromocenters and have the capacity to promote chromatin condensation [28, 45]. Histone H1 in *Arabidopsis* was recently reported to induce formation of heterochromatic foci via phase separation mediated by its C-terminal IDR [17]. Thus, H2B.8 maybe deposited to chromocenters *via* dimer formation with H2A.W.12, and its function in chromatin aggregation might be facilitated by other nuclear factors such as histone H1 [9, 17] as well as the AT-hook protein (encoded by At1g48610) whose function is presently unknown. The AT-hook is a small DNA-binding motif first identified in high mobility group (HMG) of non-histone proteins and later in multiple chromosomal/DNA-binding proteins involved in chromatin structure and function

[2]. The finding that in *ddm1* protoplasts H2B.8-GFP was mis-localized suggests that deposition of H2B.8 at chromocenters may be directly control by association with DDM1 or indirectly via the requirement for DNA methylation or H3K9 methylation. This may be supported by the finding that DDM1 often showed localization to chromocenters [47] and H2A.W deposition at heterochromatic, TE-rich regions is mediated by DDM1 [28]. The association of H2B.8 with H2A.X.3 is puzzling since H2A.X variants have been reported to occupy the body of active genes (Lei & Berger, 2019) and undergo rapid phosphorylation at sites of DNA double-strand breaks to initiate DNA repair [32]. Thus, nucleosomes composed of H2B.8-H2A.X.3 dimers may characterize chromatin aggregates that are transcriptionally active [10, 39].

H2B.8 SUMOylation

Our analysis showed that all H2B variants fused to GFP expressed under the constitutive 35 S promoter are assembled into nucleosome and could be extracted from nuclei by increasing salt concentration similarly to the reference dimethylated H3K4 or ubiquitinated H2B. Interestingly, three isoforms of H2B.8-GFP could be recovered at positions corresponding to ~54, 64 and 75 kDa. Our analysis clearly showed that one isoform at about 64 kDa is SUMOylated and can be identified by antibodies raised to SUMO1/SUMO3. Notably, comprehensive analysis of SUMOylated proteins in *Arabidopsis* revealed that most proteins are nuclear and include the histone H2B variant, H2B.9 that is modified by SUMO at K142 [33]. However, the analysis of H2B.9-GFP in transgenic plants showed a single protein corresponding to the expected molecular weight of H2B.9-GFP (~45 kDa) and a slow migrating H2B.9-GFP isoform could not be observed. This could be explained by the low level of H2B.9-GFP undergoing SUMOylation, or H2B.9 SUMOylation is induced following exposure to stress [3] or that the GFP protein renders K142 of H2B.9 inaccessible for SUMOylation. The role played by SUMO in H2B.8 nuclear distribution and function is currently under study. However, it is assumed that protein SUMOylation may affect its interaction with other proteins as well as with proteins carrying SUMO-interacting motifs (SIMs). Interestingly, H2B.8 possesses SIM at its N-terminal extension (8-VVSV-11) which may serve as a binding site for SUMOylated H2B.8. Thus, it is plausible that SUMOylation of H2B.8 may allow for H2B.8-H2B.8 interaction and assisted by other nuclear factors (e.g., histone H1; He et al., [17] bringing nucleosomes into proximity to facilitate chromatin aggregation. Alternatively, SUMOylation of H2B.8 may allow tethering of H2B.8-containing chromatin to the nuclear periphery, a subject currently studied.

H2B variants and flowering

We showed that H2B variants have a notable effect on flowering time under long day photoperiod. Thus, expression under the 35 S promoter of H2B.5 and H2B.9, but not of H2B.8 resulted in early flowering, while mutation of H2B.5 gene resulted in late flowering compared to wild type plants. Previous studies showed that H2B has a role in flowering time. Monoubiquitination of H2B, commonly associated with permissive chromatin is linked to repression of the transition to flowering [15], while impairment of H2B ubiquitination promoted early flowering [11]; the specific H2B variants involved in regulating flowering time have not been explored yet. Notably, all H2B variants, except H2B.8 in *Arabidopsis* share high amino acid sequence homology at their C terminus and the ubiquitination site is highly conserved.

Various histone variants have been implicated in controlling flowering in Arabidopsis. The expression of the FLOWERING LOCUS C (FLC) gene, a central repressor of the transition to flowering requires the H2A.Z variant since reduced deposition of H2A.Z in chromatin has led to reduced FLC expression and premature flowering [13]. Also, the non-replicative H3.3 variant in Arabidopsis was shown to act in flowering repression. It accumulates at the FLC locus to maintain its permissive state *via* histone H3 methylation at lysine 4 and 36 [50]. Hence, it is presumed that deposition of H2B.5 and or H2B.9 at certain flowering loci negate the effects of H3.3 and H2A.Z variants to bring about flowering. More research is needed to determine the H2A variants capable of dimerization with H2B.5 and H2B.9 and whether they operate as negative or positive regulators of flowering genes.

Supplementary Information

The online version contains supplementary material available at https://doi.org/10.1186/s12870-024-05532-4.

Supplementary Material 1

Supplementary Material 2

Acknowledgements

We thank Ferenc Nagy for providing Arabidopsis seeds of transgenic phyB-GFP. We also thank Noga Sikron-Persi for her assistance in confocal microscopy analysis. This research was supported by the Israel Science Foundation to GG.

Author contributions

GG and JK planed and designed the research; JK, generated transgenic plants; TVS and SS performed protoplasts transformation; JK, VST, SS, JRS, RG, AP, NN and ZAA performed experiments, analyzed, and interpreted the data. GG wrote the manuscript. JK and VST contributed equally to the work. All authors have read and approved the manuscript.

Funding

This research was supported by the Israel Science Foundation No. 667/19 to GG.

Data availability

Data is provided within the manuscript or supplementary information files.

Declarations

Ethical approval
Not applicable.

Consent for publication
Not applicable.

Competing interests
The authors declare no competing interests.

Received: 16 May 2024 / Accepted: 21 August 2024
Published online: 28 August 2024

References

1. Amiad-Pavlov D, Lorber D, Bajpai G, Reuveny A, Roncato F, Alon R, Safran S, Volk T. Live imaging of chromatin distribution reveals novel principles of nuclear architecture and chromatin compartmentalization. Sci Adv. 2021;7:eabf6251. https://doi.org/10.1126/sciadv.abf6251.
2. Aravind L, Landsman D. AT-hook motifs identified in a wide variety of DNA-binding proteins. Nucleic Acids Res. 1998;26:4413–21. https://doi.org/10.1093/nar/26.19.4413.
3. Augustine RC, Vierstra RD. SUMOylation: re-wiring the plant nucleus during stress and development. Curr Opin Plant Biol. 2018;45:143–54. https://doi.org/10.1016/j.pbi.2018.06.006.
4. Bartee L, Malagnac F, Bender J. Arabidopsis cmt3 chromomethylase mutations block non-CG methylation and silencing of an endogenous gene. Genes Dev. 2001;15:1753–8. https://doi.org/10.1101/gad.905701.
5. Bergmüller E, Gehrig PM, Gruissem W. Characterization of post-translational modifications of histone H2B-variants isolated from *Arabidopsis thaliana*. J Proteome Res. 2007;6:3655–68. https://doi.org/10.1021/pr0702159.
6. Borcherds W, Bremer A, Borgia MB, Mittag T. How do intrinsically disordered protein regions encode a driving force for liquid-liquid phase separation? Curr Opin Struct Biol. 2021;67:41–50. https://doi.org/10.1016/j.sbi.2020.09.004.
7. Borg M, Berger F. Chromatin remodelling during male gametophyte development. Plant J. 2015;83:177–88. https://doi.org/10.1111/tpj.12856.
8. Bourbousse C, Ahmed I, Roudier F, Zabulon G, Blondet E, Balzergue S, Colot V, Bowler C, Barneche F. Histone H2B monoubiquitination facilitates the rapid modulation of gene expression during Arabidopsis photomorphogenesis. PLoS Genet. 2012;8:e1002825. https://doi.org/10.1371/journal.pgen.1002825.
9. Bourguet P, Picard CL, Yelagandula R, Pélissier T, Lorković ZJ, Feng S, Pouch-Pélissier MN, Schmücker A, Jacobsen SE, Berger F, Mathieu O. The histone variant H2A.W and linker histone H1 co-regulate heterochromatin accessibility and DNA methylation. Nat Comm. 2021;12:2683. https://doi.org/10.1038/s41467-021-22993-5.
10. Buttress T, He S, Wang L, Zhou S, Saalbach G, Vickers M, Li G, Li P, Feng X. Histone H2B.8 compacts flowering plant sperm through chromatin phase separation. Nature. 2022;611:614–22. https://doi.org/10.1038/s41586-022-05386-6.
11. Cao Y, Dai Y, Cui S, Ma L. Histone H2B monoubiquitination in the chromatin of FLOWERING LOCUS C regulates flowering time in Arabidopsis. Plant Cell. 2008;20:2586–602. https://doi.org/10.1105/tpc.108.062760.
12. Chaboute ME, Chaubet N, Gigot C, Philipps G. Histones and histone genes in higher plants: structure and genomic organization. Biochimie. 1993;75(7):523–31. https://doi.org/10.1016/0300-9084(93)90057-y.
13. Deal RB, Topp CN, McKinney EC, Meagher RB. Repression of flowering in Arabidopsis requires activation of FLOWERING LOCUS C expression by the histone variant H2A.Z. Plant Cell. 2007;19:74–83. https://doi.org/10.1105/tpc.106.048447.
14. Fass E, Shahar S, Zhao J, Zemach A, Avivi Y, Grafi G. Phosphorylation of histone H3 at serine 10 cannot account directly for the detachment of human heterochromatin protein 1gamma from mitotic chromosomes in plant cells. J Biol Chem. 2002;277:30921–7. https://doi.org/10.1074/jbc.M112250200.
15. Gu X, Jiang D, Wang Y, Bachmair A, He Y. Repression of the floral transition via histone H2B monoubiquitination. Plant J. 2009;57:522–33. https://doi.org/10.1111/j.1365-313X.2008.03709.x.
16. Hansen JC, Maeshima K, Hendzel MJ. The solid and liquid states of chromatin. Epigenetics Chromatin. 2021;14:50. https://doi.org/10.1186/s13072-021-00424-5.
17. He S, Yu Y, Wang L, Zhang J, Bai Z, Li G, Li P, Feng X. Linker histone H1 drives heterochromatin condensation via phase separation in Arabidopsis. Plant Cell. 2024;36:1829–43. https://doi.org/10.1093/plcell/koae034.
18. Himanen K, Woloszynska M, Boccardi TM, De Groeve S, Nelissen H, Bruno L, Vuylsteke M, Van Lijsebettens M. Histone H2B monoubiquitination is required to reach maximal transcript levels of circadian clock genes in Arabidopsis. Plant J. 2012;72:249–60. https://doi.org/10.1111/j.1365-313X.2012.05071.x.
19. Hu B, Wang N, Bi X, Karaaslan ES, Weber AL, Zhu W, Berendzen KW, Liu C. Plant lamin-like proteins mediate chromatin tethering at the nuclear periphery. Genome Biol. 2019;20:87. https://doi.org/10.1186/s13059-019-1694-3.
20. Jiang D, Borg M, Lorković ZJ, Montgomery SA, Osakabe A, Yelagandula R, Axelsson E, Berger F. The evolution and functional divergence of the histone H2B family in plants. PLoS Genet. 2020;16:e1008964. https://doi.org/10.1371/journal.pgen.1008964.
21. Khadka J, Pesok A, Grafi G. Plant histone HTB (H2B) variants in regulating chromatin structure and function. Plants. 2020;9:1435. https://doi.org/10.3390/plants9111435.
22. Lei B, Berger F. H2A variants in *Arabidopsis*: versatile regulators of genome activity. Plant Comm. 2019;1:100015. https://doi.org/10.1016/j.xplc.2019.100015.
23. Li B, Carey M, Workman JL. The role of chromatin during transcription. Cell. 2007;128:707–19. https://doi.org/10.1016/j.cell.2007.01.015.
24. Li M, Fang Y. Histone variants: the artists of eukaryotic chromatin. Sci China Life Sci. 2015;58:232–9. https://doi.org/10.1007/s11427-015-4817-4.
25. Lindroth AM, Cao X, Jackson JP, Zilberman D, McCallum CM, Henikoff S, Jacobsen SE. Requirement of CHROMOMETHYLASE3 for maintenance of CpXpG methylation. Science. 2001;292:2077–80. https://doi.org/10.1126/science.1059745.
26. Medzihradszky M, Bindics J, Ádám É, Viczián A, Klement É, Lorrain S, Gyula P, Mérai Z, Fankhauser C, Medzihradszky KF, Kunkel T, Schäfer E, Nagy F. Phosphorylation of phytochrome B inhibits light-induced signaling via accelerated dark reversion in Arabidopsis. Plant Cell. 2013;25:535–44. https://doi.org/10.1105/tpc.112.106898.
27. Murashige T, Skoog F. A revised medium for rapid growth and bio assays with tobacco tissue cultures. Plant Physiol. 1962;15:473–97. https://doi.org/10.1111/j.1399-3054.1962.tb08052.x.
28. Osakabe A, Jamge B, Axelsson E, Montgomery SA, Akimcheva S, Kuehn AL, Pisupati R, Lorković ZJ, Yelagandula R, Kakutani T, Berger F. The chromatin remodeler DDM1 prevents transposon mobility through deposition of histone variant H2A.W. Nat Cell Biol. 2021;23:391–400. https://doi.org/10.1038/s41556-021-00658-1.
29. Probst AV, Desvoyes B, Gutierrez C. Similar yet critically different: the distribution, dynamics and function of histone variants. J Exp Bot. 2020;71:5191–204. https://doi.org/10.1093/jxb/eraa230.
30. Remboutsika E, Lutz Y, Gansmuller A, Vonesch JL, Losson R, Chambon P. The putative nuclear receptor mediator TIF1alpha is tightly associated with euchromatin. J Cell Sci. 1999;112:1671–83. https://doi.org/10.1242/jcs.112.11.1671.
31. Robinson PJ, Rhodes D. Structure of the '30 nm' chromatin fibre: a key role for the linker histone. Curr Opin Struct Biol. 2006;16:336–43. https://doi.org/10.1016/j.sbi.2006.05.007.
32. Rogakou EP, Pilch DR, Orr AH, Ivanova VS, Bonner WM. DNA double-stranded breaks induce histone H2AX phosphorylation on serine 139. J Biol Chem. 1998;273:5858–68. https://doi.org/10.1074/jbc.273.10.5858.
33. Rytz TC, Miller MJ, McLoughlin F, Augustine RC, Marshall RS, Juan YT, Charng YY, Scalf M, Smith LM, Vierstra RD. SUMOylome Profiling reveals a diverse array of nuclear targets modified by the SUMO ligase SIZ1 during heat stress. Plant Cell. 2018;30:1077–99. https://doi.org/10.1105/tpc.17.00993.
34. Sakamoto K, Nagatani A. Nuclear localization activity of phytochrome B. Plant J. 1996;10:859–68. https://doi.org/10.1046/j.1365-313x.1996.10050859.x.
35. Saxena PK, Fowke LC, King J. An efficient procedure for isolation of nuclei from plant protoplasts. Protoplasma. 1985;128:184–9. https://doi.org/10.1007/BF01276340.
36. Shilatifard A. Chromatin modifications by methylation and ubiquitination: implications in the regulation of gene expression. Annu Rev Biochem. 2006;75:243–69. https://doi.org/10.1146/annurev.biochem.75.103004.142422.
37. Soppe WJ, Jasencakova Z, Houben A, Kakutani T, Meister A, Huang MS, Jacobsen SE, Schubert I, Fransz PF. DNA methylation controls histone H3 lysine 9 methylation and heterochromatin assembly in Arabidopsis. EMBO J. 2002;21:6549–59. https://doi.org/10.1093/emboj/cdf657.
38. Sridhar VV, Kapoor A, Zhang K, Zhu J, Zhou T, Hasegawa PM, Bressan RA, Zhu JK. Control of DNA methylation and heterochromatic silencing by histone

H2B deubiquitination. Nature. 2007;447:735–8. https://doi.org/10.1038/nature05864.
39. Tse C, Sera T, Wolffe AP, Hansen JC. Disruption of higher-order folding by core histone acetylation dramatically enhances transcription of nucleosomal arrays by RNA polymerase III. Mol Cell Biol. 1998;18:4629–38. https://doi.org/10.1128/MCB.18.8.4629.
40. Tyanova S, Temu T, Sinitcyn P, Carlson A, Hein MY, Geiger T, Mann M, Cox J. The Perseus computational platform for comprehensive analysis of (prote)omics data. Nat Methods. 2016;13:731–40. https://doi.org/10.1038/nmeth.3901.
41. van Zanten M, Koini MA, Geyer R, Liu Y, Brambilla V, Bartels D, Koornneef M, Fransz P, Soppe WJ. Seed maturation in Arabidopsis thaliana is characterized by nuclear size reduction and increased chromatin condensation. Proc Natl Acad Sci U S A. 2011;108:20219–24. https://doi.org/10.1073/pnas.1117726108.
42. Vongs A, Kakutani T, Martienssen RA, Richards EJ. Arabidopsis thaliana DNA methylation mutants. Science. 1993;260:1926–8. https://doi.org/10.1126/science.8316832.
43. Walsh I, Martin AJ, Di Domenico T, Tosatto SC. ESpritz: accurate and fast prediction of protein disorder. Bioinformatics. 2012;28:503–9. https://doi.org/10.1093/bioinformatics/btr682.
44. Yamaguchi R, Nakamura M, Mochizuki N, Kay SA, Nagatani A. Light-dependent translocation of a phytochrome B-GFP fusion protein to the nucleus in transgenic Arabidopsis. J Cell Biology. 1999;145:437–45. https://doi.org/10.1083/jcb.145.3.437.
45. Yelagandula R, Stroud H, Holec S, Zhou K, Feng S, Zhong X, Muthurajan UM, Nie X, Kawashima T, Groth M, Luger K, Jacobsen SE, Berger F. The histone variant H2A.W defines heterochromatin and promotes chromatin condensation in Arabidopsis. Cell. 2014;158:98–109. https://doi.org/10.1016/j.cell.2014.06.006.
46. Yoo SD, Cho YH, Sheen J. Arabidopsis mesophyll protoplasts: a versatile cell system for transient gene expression analysis. Nat Protoc. 2007;2:1565–72. https://doi.org/10.1038/nprot.2007.199.
47. Zemach A, Li Y, Wayburn B, Ben-Meir H, Kiss V, Avivi Y, Kalchenko V, Jacobsen SE, Grafi G. DDM1 binds Arabidopsis methyl-CpG binding domain proteins and affects their subnuclear localization. Plant Cell. 2005;17:1549–58. https://doi.org/10.1105/tpc.105.031567.
48. Zemach A, Gaspan O, Grafi G. The three methyl-CpG-binding domains of AtMBD7 control its subnuclear localization and mobility. J Biol Chem. 2008;283:8406–11. https://doi.org/10.1074/jbc.M706221200.
49. Zhang X, Henriques R, Lin SS, Niu QW, Chua NH. Agrobacterium-mediated transformation of Arabidopsis thaliana using the floral dip method. Nat Protoc. 2006;1:641–6. https://doi.org/10.1038/nprot.2006.97.
50. Zhao F, Zhang H, Zhao T, Li Z, Jiang D. The histone variant H3.3 promotes the active chromatin state to repress flowering in Arabidopsis. Plant Physiol. 2021;186:2051–63. https://doi.org/10.1093/plphys/kiab224.
51. Zhao J, Morozova N, Williams L, Libs L, Avivi Y, Grafi G. Two phases of chromatin decondensation during cellular dedifferentiation of plant cells: distinction between competence for cell-fate switch and a commitment for S phase. J Biol Chem. 2001;276:22772–8.

Publisher's note

Springer Nature remains neutral with regard to jurisdictional claims in published maps and institutional affiliations.